Materials Research Proceedings 44 (2024) 718-735 https://doi.org/10.21741/9781644903254-77

Microstructure evolution of semi-solid billet fabricated by semi-solid isothermal heat treatment of wrought AlSi7Mg aluminum alloy

JIANG Jufu[1,a *], SONG Tao[2], WANG Ying[2,b *], ZHANG Ying[1], ZHU Liang[1] and DONG Jian[1]

[1]School of Materials Science and Engineering, Harbin Institute of Technology, Harbin, 150001, P.R. China

[2]School of Mechatronics Engineering, Harbin Institute of Technology, Harbin, 150001, P.R. China

[a]jiangjufu@hit.edu.cn, [b]wangying1002@hit.edu.cn

Keywords: Semi-Solid, Isothermal Heat Treatment, Microstructure, AlSi7Mg Aluminum Alloy

Abstract: In this paper, the as-cast AlSi7Mg aluminum alloy billet was upsetted above recrystallization temperature to obtain wrought aluminum alloy with 50% deformation degree, and semi-solid isothermal treatment method was employed to achieve semi-solid billet of the wrought AlSi7Mg aluminum alloy. The microstructure observation and evolution law were investigated via optical microscope and scanning electron microscope. The results show that the primary α-Al phase can be changed from dendrite to spherical structure by semi-solid isothermal treatment of the wrought alloy (SSITWA). The complete transformation of the primary α-Al phase from dendrite to spherical structure can be achieved by increasing the isothermal temperature and prolongation of holding time. However, when the holding time is too long, the spheroidized grains will grow abnormally and eventually become irregularly shaped grains. High isothermal temperature can increase the primary α-Al size and reduce the time of dendrite to spheroidal grains. The average grain size of AlSi7Mg aluminum alloy semi-solid billet fabricated by SSITWA varies in a range of from 15 μm to 65 μm when the temperature and holding time change. The content of Al and Si elements in primary α-Al phase is obviously higher than that in liquid eutectic phase consisting of Al and Si elements, and the distribution of Mg element is uniform in the microstructure of semi-solid billet fabricated by SSITWA.

Introduction

AlSi7Mg aluminum alloy is a hypoeutectic alloy with silicon and magnesium as the main alloying elements. Because of the large amount of Al-Si eutectic, large temperature interval of solidus and liquidus and good fluidity, it is a desirable alloy for semi-solid metal forming [1]. It is attractive in the automotive and aerospace industries for its light weight and good corrosion resistance [2-5]. AlSi7Mg aluminum alloy also has good mechanical strength, ductility, fatigue properties, and machinability [6-8].

Semi-solid processing technology is a kind of advanced forming technology combining liquid metal casting and solid metal plastic processing [9-12]. It is widely used in aluminum alloy processing [13, 14]. The primary process of semi-solid processing is to prepare semi-solid slurry (billet) with spherical grains and thixotropic property [15]. At present, there are many preparation methods of slurry, including mechanical stirring (MS) method, electromagnetic stirring (ES) method, ultrasonic treatment (UT) method, strain induced melt activation method (SIMA) and recrystallization and partial remelting method (RAP) [16-18]. Many scholars have carried out relevant research based on fabrication of semi-solid slurry of aluminum alloys. Jiang et al.[19] proposed a novel method for fabricating semi-solid billet of aluminum alloy, named semi-solid

isothermal treatment of wrought alloy (SSITWA). It involves a partial melting of industrial wrought aluminum alloy (hot-rolled plate or hot-extrusion bar). Four kinds of deformed aluminum alloys were prepared and then the thixoforming experiments were carried out on four typical parts. The results further confirmed the feasibility of thixoforming route of short process. Guan et al.[20] studied the microstructure and mechanical properties of rheological castings of 7075 alloy treated by annular electromagnetic stirring melt. The results showed that the degree of refinement and uniformity of solidification structure could be significantly improved under such conditions. The slurry was used for subsequent rheological casting, and the hot crack defects in the casting process were significantly alleviated. Liu et al. [21] prepared a high strength Al-6Si-6Cu semi-solid billet by liquid phase reaction sintering. The results showed that Cu nanoparticles precipitated in Al grains of the Al-6Si-6Cu (wt%) semi-solid billet and showed strong pinning effect. Under this condition, the Al-6Si-6Cu semi-solid billet yield strength (YS) and ultimate strength (US) increased by 120% and 67.4%. Zhang et al. [22] studied the microstructure evolution of an Al-Si alloy during shear-vibration coupling sub-rapid solidification and the effects of three key parameters, i.e., pouring temperature, vibration frequency, and tilting angle of the slope plate on the microstructure. The results showed that compared with the traditional solidification on the cooling slope plate, more dissociated grains can be produced rapidly by the debonding with the plate surface. The additional vibration would make the dissociated grains more susceptible to subsequent diffusion and would also generate smaller, more uniform primary grains. Yu et al. [23] prepared rare-earth praseodymium cerium (Pr/Ce) reinforced semi-solid ADC12 slurry by high-energy ultrasonic method. The effects of solid fraction, ultrasonic power and Pr/Ce addition on the steady-state apparent viscosity of slurry at a certain shear rate were investigated.. The results showed that the apparent viscosity and solid phase fraction of semi-solid ADC12 slurry increased with the addition of Pr/Ce, but the ultrasonic power was opposite. At the same time, high energy ultrasound also played a role in grain refinement. Semi-solid isothermal heat treatment of wrought aluminum (SSITWA) is that the alloy billet is first subjected to a certain thermal deformation process, and then the semi-solid isothermal treatment is carried out to transform the dendrite structure into spheroidized structure. Then the semi-solid forming process is carried out. The process of non-dendrite ingot billet preparation is omitted as compared to MS, ES and UT methods, and it reduces the cold working process at room temperature as compared to SIMA method. It also reduces the resistance to formation of material as compared to RAP. Therefore, this method has the advantages of short process flow, simple equipment and high operability, and it provides a new idea for the preparation of aluminum alloy semi-solid billet.

In this study, AlSi7Mg semi-solid aluminum alloy billets were prepared by semi-solid isothermal heat treatment of wrought alloy (SSITWA) in order to shorten the working hours of semi-solid billets. The wrought AlSi7Mg alloy was prepared by upsetting with a severe plastic deformation above recrystallization temperature, and isothermal treatment experiments were carried out at different isothermal temperatures and holding time. By microstructure observation and energy spectrum analysis of the semi-solid billet, the influence of process parameters on microstructure of the semi-solid billet was quantitatively analyzed with the average grain size and average shape factor. The microstructure evolution of AlSi7Mg aluminum alloy under the semi-solid temperature range isothermal treatment was determined.

Experimental procedure

In this Study, AlSi7Mg aluminum alloy semi-solid billets were prepared by SSITWA. First, the hot upsetting experiment was carried out on AlSi7Mg alloy, then the intermediate billets were prepared under the selected parameters, and the isothermal treatment experiments were carried out at different isothermal temperatures and holding time.

Experimental material. The commercial AlSi7Mg aluminum alloy bar was used as the feedstock, with a chemical composition shown in Table 1. The solidus and liquidus temperatures were determined by STA449F3 differential scanning calorimeter (DSC). 3 mm diameter and 1.5 mm height disc sample was heated in an argon atmosphere at a rate of 10℃ min^{-1} from room temperature to 700℃. According to the DSC result [24], the solidus temperature was 574.5℃, and liquidus temperature was 636.2℃, indicating a wide range of semi-solid state. The solid fractions at semi-solid isothermal temperatures 590℃, 595℃, 600℃, 605℃ and 610℃ were 0.64, 0.55, 0.491, 0.433 and 0.367, respectively [24].

Table 1. Chemical composition of AlSi7Mg alloy (wt.%).

Si	Mg	Ti	Fe	Mn	Cu	Zn	Al
6.930	0.490	0.054	0.020	0.033	0.011	0.043	Bal.

Semi-solid isothermal treatment of wrought AlSi7Mg alloy. The equipment used in the experiment was 50000 kN hydraulic press and box-type resistance heating furnace. 120 mm×160 mm original ingot was heated to 150℃ in a heating furnace and sprayed with a lubricant of water-based graphite. After the billet was heated to 350℃, it was upsetted on a press at a deformation rate of about 80 mm/min, and the upsetting process was stopped until the deformation reached 50%. Finally, the drum-shaped billet was obtained. The cuboid specimens with 10*10*12 mm^3 for semi-solid isothermal treatment experiment were cut from the upsetted billet. The semi-solid isothermal temperatures were 590℃, 595℃, 600℃, 605℃ and 610℃, and the holding time was 1 min, 5 min, 10 min, 15 min and 20 min, respectively. 0.5% HF solution was used for corrosion treatment, and the corrosion time was 5~10 s. There were 25 groups of experimental parameters. The samples were isothermal treated with a box-type resistance heating furnace (temperature accuracy ± 1 ℃). The samples were heated to a specified temperature and held for a set time. Then the samples were taken out from the box-type resistance furnace and quenched in water to retain the microstructure under this parameter. The specific parameters of semi-solid isothermal treatment are shown in Table 2. The experimental flow chart is shown in Fig. 1.

Table 2. Experimental parameters of AlSi7Mg alloy isothermal treatment.

NO.	temperature / ℃	holding time /min	NO.	temperature / ℃	holding time /min
1	590	1	16	605	1
2	590	5	17	605	5
3	590	10	18	605	10
4	590	15	19	605	15
5	590	20	20	605	20
6	595	1	21	610	1
7	595	5	22	610	5
8	595	10	23	610	10
9	595	15	24	610	15
10	595	20	25	610	20
11	600	1			
12	600	5			
13	600	10			
14	600	15			
15	600	20			

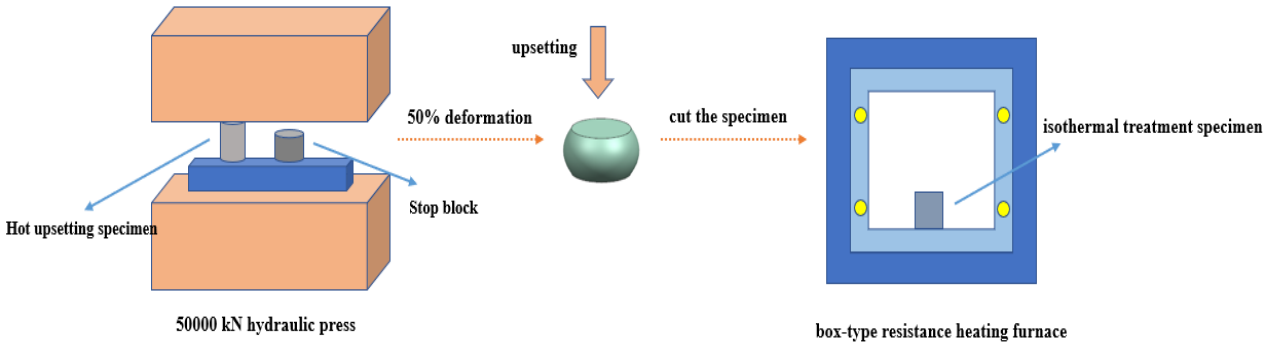

Fig. 1. Experimental flow chart.

After the isothermal treatment, the samples were ground with 200, 400, 800, 1200, 1500, and 2000 grit SiC sandpapers, and they were polished and corroded by polishing machine and 0.5% HF etchant. The metallographic images were taken by an optical microscopy (Olympus GX71). Image Pro Plus software was used to analyze and process the metallographic images (no less than 300 grains were measured in order to reduce statistical error). The area and perimeter of the grains were counted, and the average grain size was calculated. The average shape factor was used to describe the roundness of the grains. The calculation method was shown in formulas (1) and (2), respectively [25]:

$$D=\frac{1}{N}\sum_{i=1}^{N}\sqrt{\frac{4A_i}{\pi}} \quad (1)$$

$$f=\frac{1}{N}\sum_{i=1}^{N}\frac{4\pi A_i}{P_i^2} \quad (2)$$

Where, D——Average grain size/μm;
f——Average shape factor;
A_i——The area of the ith grain or grain measured;
P_i——The circumference of the ith grain or grain measured;
N——The total number of grains or grains measured.

Results and Discussion

Microstructure evolution of AlSi7Mg Al alloy during semi-solid isothermal treatment. Fig. 2 to Fig. 6 show the metallographic images of AlSi7Mg alloy in different temperature groups with an increase of soaking time. The grey colour part represents primary α-Al grain and the black colour part represents liquid phase, i.e. low-melting-point eutectic structure. Fig. 2 shows the microstructure of AlSi7Mg alloy held at 590℃ for 1 min, 5 min, 10 min, 15 min and 20 min. Fig. 2(a) shows the microstructures of AlSi7Mg alloy held at 590℃ for 1 min. Due to the short holding time, the dendrites in the original as-cast structure still existed. After holding at 590℃ for 1 min, the dendrite grains were relatively coarse and the intergranular liquid phases were less. Only a small number of eutectic phases melted, and no liquid phases appeared in the grains. The morphology of eutectic phases did not change much. This is because that solid-liquid transition depends on solute diffusion and the solute diffusion requires enough time at a constant temperature. In the early stage of semi-solid isothermal treatment, the soaking time is too short to ensure enough time of solute diffusion. As a result, the microstructure still exhibits a dendrite morphology. Fig. 2(b) shows the microstructures with a holding time of 5 min. With the increase of holding time, the grain size became uniform, and the particles became fine and spheroidization occurred. A small number of liquid phases began to appear in the grain, most of the eutectic phases

on the α phase grain boundary had melted into liquid phases. But it is found that a small amount of granulated eutectic phases had not melted. The α-Al phase was basically spheroidized, and the adjacent grains merged and grew up. The increase of holding time was beneficial to the formation of spherical grains and the melting of eutectic phases.

Fig. 2(c) shows the microstructures of AlSi7Mg alloy after holding for 10 min. It could be seen that the grains had obvious signs of growth. With the increase of holding time, the grains became larger and larger after merging, and the liquid phases in the grains also became more and more, which tended to melt from the inside. Grains began to break down at grain boundaries to form small grains, which became new grains and grew up. Under the joint action of interface curvature and interface energy, small grains were gradually engulfed by large grains and the large grains kept growing. Fig. 2(d) shows the microstructures of AlSi7Mg alloy with a holding time of 15 min. The ratio of liquid phases was relatively high, the distance between adjacent large grains was far. A large number of fine grains generated by the grain breakage in the previous stage were distributed between the liquid phases. The rose-shape appeared between grains in the region with less liquid phases due to their close grain orientation and merger growth. Because of the liquid phase wrapping, the large grains were concave inward to form rosette and had the tendency of breaking into new grains. Fig. 2(e) shows the microstructures of AlSi7Mg alloy after holding for 20 min. Most of the rose-like dendrites were melted. Traces of original rose-like grains could be seen from the microstructure. The burrs previously formed by grain and grain boundary fragmentation had grown and spheroidized and new burrs were also being formed. Grown burr grains had smooth rounded edges.

As can be seen from the changes of the microstructures at different temperatures with changing time, when the isothermal temperature was 590℃ and the holding time was less than 5 min, the microstructures first grew from dendrites and gradually broke into clumps or particles at the root with the increase of the holding time. With the further increase of holding time, Al grains grew from granular or massive, and part of them became rose-shaped and then fragmented into spherical and massive again. In this process, the distribution of eutectic structure became more uniform. It can be concluded that the microstructures evolution of semi-solid isothermal treatment process was as follows: (1) dendrite growth, (2) massive or granular, (3) rosette, (4) fragmentary massive or granular, (5) spheroidization, (6) grain growth.

Materials Research Proceedings 44 (2024) 718-735 https://doi.org/10.21741/9781644903254-77

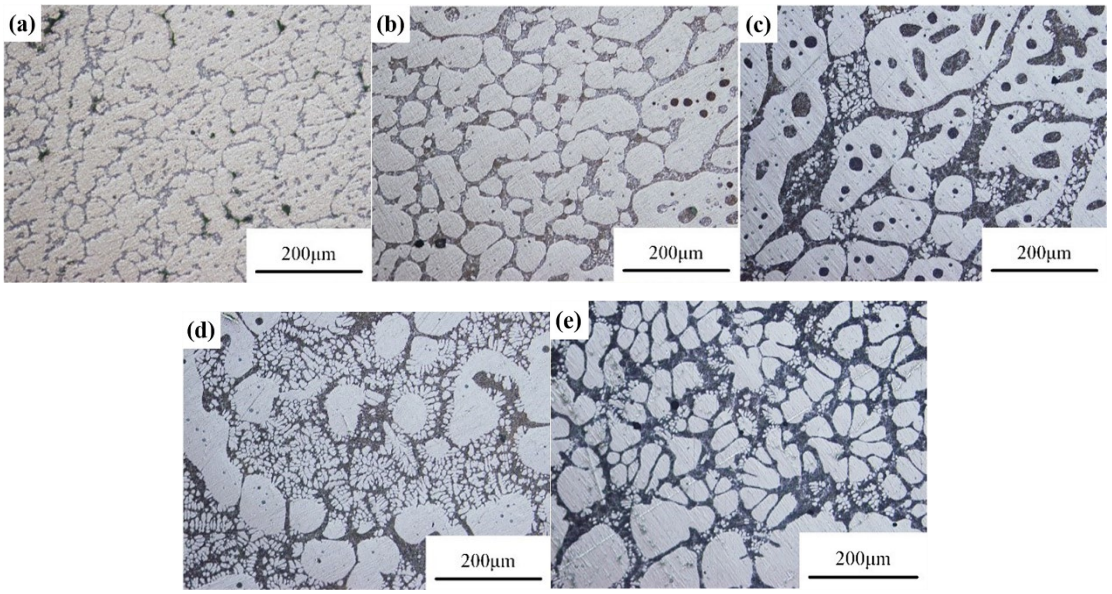

Fig. 2. Microstructure images of AlSi7Mg alloy held at 590℃ for different time: (a) 1 min; (b) 5 min; (c) 10 min; (d) 15 min; (e) 20 min.

Fig. 3 shows the microstructures of AlSi7Mg alloy after holding at 595℃ for different time. Fig. 3(a) shows the microstructures of AlSi7Mg alloy after holding at 595℃ for 1 min. The grains were coarse, with more coarse dendrites and less intergranular liquid phases, and there was bond between grains. Fig. 3(b) shows the microstructures of AlSi7Mg alloy after holding at 595℃ for 5 min. Combined growth of adjacent grains appeared, and some of the dendrite melted into an independent dendrite arm due to their proximity to each other. Some of the dendrites were broken to form new grains with small size and good roundness. Fig. 3(c) shows the microstructures of AlSi7Mg alloy after holding at 595℃ for 10 min. Intergranular liquid phases increased, and ingrain liquid phases also began to appear. The new grains generated by dendrite fragmentation in the previous stage gradually grew into massive or spherical grains, and the grain boundaries of grains began to break and form a large number of burr grains. Fig. 3(d) shows the microstructures of AlSi7Mg alloy after holding at 595℃ for 15 min. The liquid phases ratio tended to be stable and mainly distributed in the intergranular area. The internal melted grains became small massive or spherical grains and grew continuously. The process of burr formation and burr growth was carried out dynamically at grain boundaries. Two or more grain boundaries of adjacent grains were connected, and there was a tendency to form rose grains. Fig. 3(e) shows the microstructures of AlSi7Mg alloy after holding at 595℃ for 20 min. At this time, the number of large grains had been greatly reduced and separated from each other, and the liquid phases were filled with small size burr grains and newly grew burr grains. The edges of large grains were rounded and smooth, and the two adjacent grains grew in “8” shape. It could be found that when the holding time was short, the microstructures and grain size were not uniform, while when the holding time was enough, the distribution of grains and eutectic phases became uniform, but the grains were coarse and round. With the increase of time, a large number of recrystallized grains (burrs) appeared at the grain edge and were in the process of dynamic generation and gradual growth. The microstructures evolution was as follows: (1) dendrite growth, (2) massive or granular, (3) rosette, (4) fragmentary massive or granular, (5) spheroidization, (6) grain growth. This was the same as the semi-solid microstructure evolution at 590 ºC for different holding time.

Materials Research Proceedings 44 (2024) 718-735 https://doi.org/10.21741/9781644903254-77

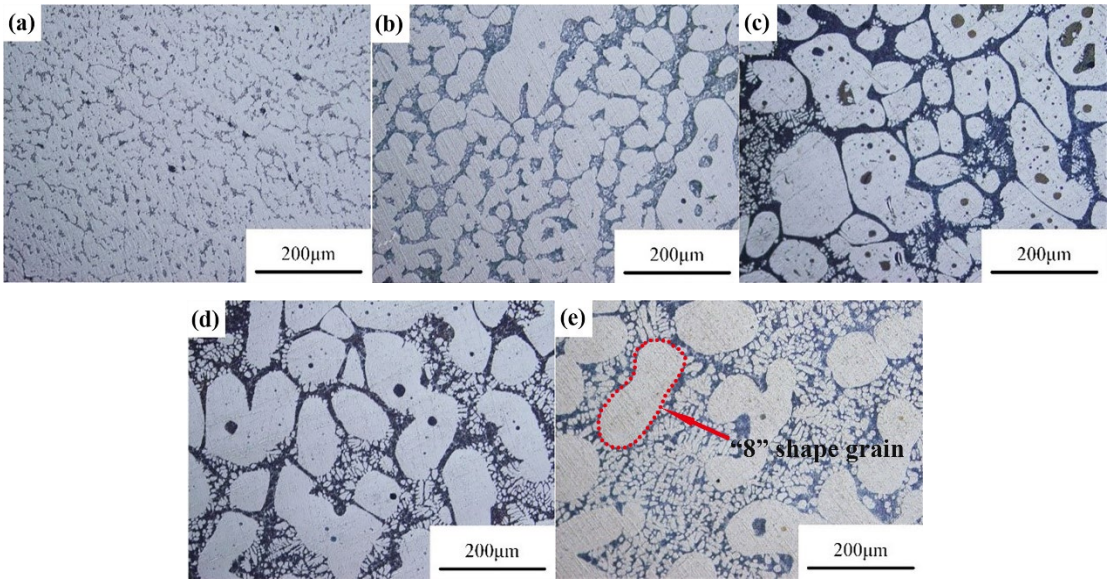

Fig. 3. Microstructure images of AlSi7Mg alloy held at 595℃ for different time: (a) 1 min; (b) 5 min; (c) 10 min; (d) 15 min; (e) 20 min.

Fig. 4 shows the microstructures of AlSi7Mg alloy after holding at 600℃ for different time. Fig. 4(a) shows the microstructures of AlSi7Mg alloy after holding at 600℃ for 1 min. Compared with the those held at 590℃ and 595℃ for 1 min, the microstructures of AlSi7Mg alloy held at 600℃ for 1 min exhibited a larger grain size. The main dendrite became wider, and the new grains formed by the melting and breaking of the dendrite arms became larger and larger. At this time, liquid phases began to form in the grain. Fig. 4(b) shows the microstructures of AlSi7Mg alloy after holding at 600℃ for 5 min. Dendrites were further broken and smaller grains were formed. The grain edges became round and spheroidized obviously. The short holding time results in a slow diffusion rate of atoms, so only a few grain boundaries appear burrs. Fig. 4(c) shows the microstructures of AlSi7Mg alloy after holding at 600℃ for 10 min. The coalescence and growth of adjacent grains increased the grain size, and the rosette grains appeared. The recrystallization of grains was obvious, and the burr grains entered the liquid phases and gradually grew up. Fig. 4(d) shows the microstructures of AlSi7Mg alloy after holding at 600℃ for 15 min. The size of the burrs generated in the previous stage increased and tended to coalesce into dendritic grains. The distance between large grains was far, and the rose grains began to break. Fig. 4(e) shows the microstructures of AlSi7Mg alloy after holding at 600℃ for 20 min. With the extension of holding time, the old rosette broke and the new rosette was formed in a dynamic equilibrium. At this time, the grain size was generally large and irregular.

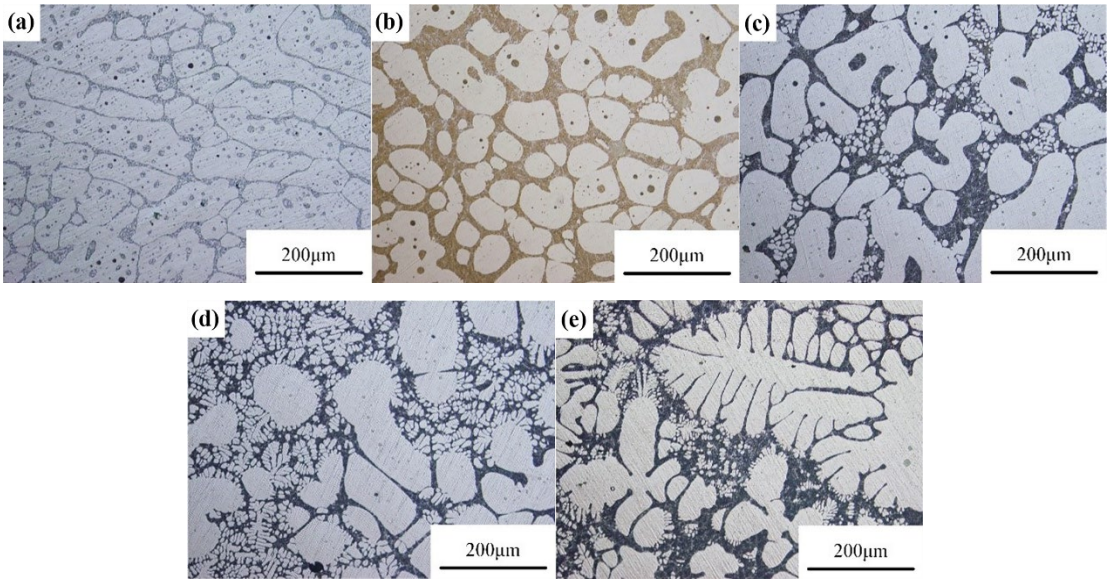

Fig. 4. Microstructure images of AlSi7Mg alloy held at 600℃ for different time: (a) 1 min; (b) 5 min; (c) 10 min; (d) 15 min; (e) 20 min.

Fig. 5 shows the microstructures of AlSi7Mg alloy after holding at 605℃ for different time. Fig. 5(a) shows the microstructures of AlSi7Mg alloy after holding at 605℃ for 1 min. Due to the reasons of atomic diffusion and energy fluctuation, the composition of the alloy would be homogenized. This would lead to the gradual coarsening of dendrites, and the disappearance of the branching characteristics of dendrites, forming clumps or grains [26]. Dendrites were encapsulated in liquid phases and began to break up into smaller grains. Traces of primitive dendrites could be seen from grain orientation. Fig. 5(b) shows the microstructures of AlSi7Mg alloy after holding at 605℃ for 5 min. The liquid phases began to appear in the grains, and the broken dendrite grains began to spheroidize. The burr grains began to break at the grain boundary. Fig. 5(c) shows the microstructures of AlSi7Mg alloy after holding at 605℃ for 10 min. There were more rosette grains in the microstructures. The burrs in the intercrystalline liquid phases grew up gradually. Fig. 5(d) shows the microstructures of AlSi7Mg alloy after holding at 605℃ for 15 min. The burrs disappeared, and the rosette grains were broken into several radial grains with larger grain size. The grains free in the liquid region were smaller and had higher roundness. Fig. 5(e) shows the microstructures of AlSi7Mg alloy after holding at 605℃ for 20 min. The grain arrangement in the region had a certain directivity. The phenomenon of adjacent grains merging and growing was not obvious. The original grains were constantly flattening and elongating.

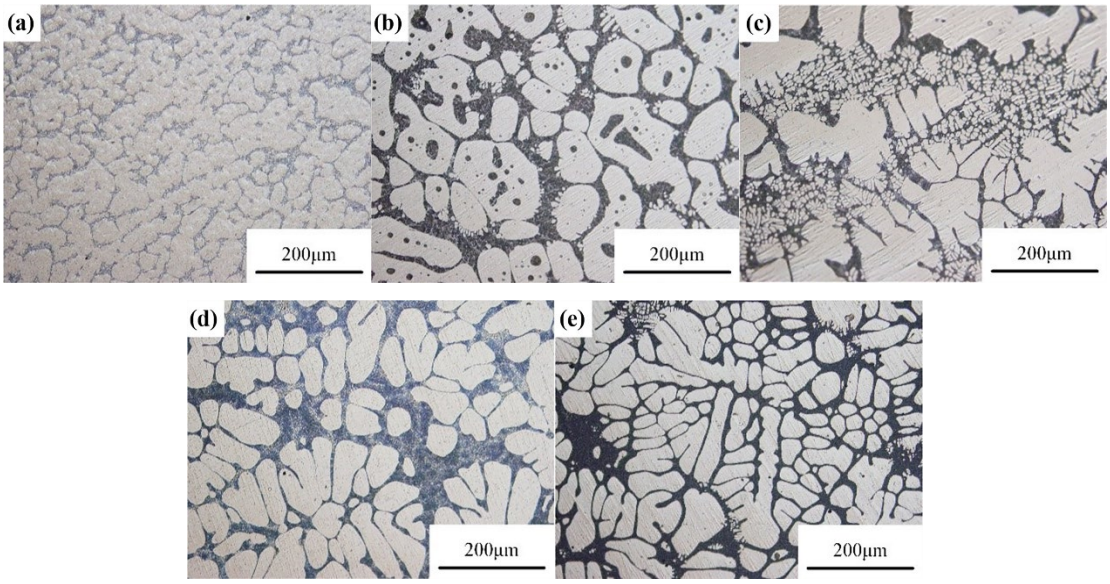

Fig. 5. Microstructure images of AlSi7Mg alloy held at 605℃ for different time: (a) 1 min; (b) 5 min; (c) 10 min; (d) 15 min; (e) 20 min.

Fig. 6 shows the microstructures of AlSi7Mg alloy after holding at 610℃ for different time. Fig. 6(a) shows the microstructures of AlSi7Mg alloy after holding at 610℃ for 1 min. Grain boundaries interpenetrated to form a network of structures. Fig. 6(b) shows the microstructures of AlSi7Mg alloy after holding at 610℃ for 5 min. A small number of spherical particles had been suspended in the liquid phases. At this time, there were both fine grains in the microstructure and large rosette grains that were about to break. Fig. 6(c) shows the microstructures of AlSi7Mg alloy after holding at 610℃ for 10 min. It could be seen that the rose-like grains without complete ripening. There were no obvious burr grains, and the structure was a large number of rose-like grains and petal grains formed after the fragmentation of rose-like grains. Fig. 6(d) shows the microstructures of AlSi7Mg alloy after holding at 610℃ for 15 min. The long grains were gradually melting off. A large number of recrystallized grains were formed at the grain boundary, and the large grains were far apart. Fig. 6(e) shows the microstructures of AlSi7Mg alloy after holding at 610℃ for 20 min. The microstructure morphology at this time was similar to that at 10 min. There were more spherical grains, but there were also many strip-like grains and fewer rose-like grains. It could be seen that the traces of the rose-like grains were broken off. But there were burr grains at the grain boundary edge.

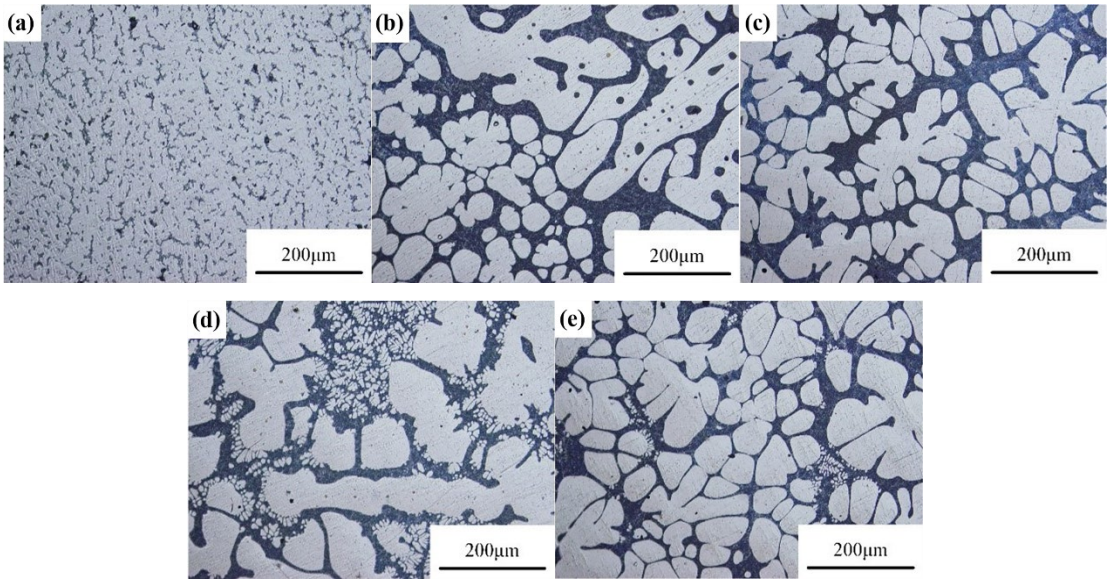

Fig. 6. Microstructure images of AlSi7Mg alloy held at 610℃ for different time: (a) 1 min; (b) 5 min; (c) 10 min; (d) 15 min; (e) 20 min.

By comparing the microstructure under the same holding time and different temperature parameters, it can be noted that the increase of isothermal temperature is helpful to accelerate the evolution of semi-solid microstructures [27]. Under the same holding time, with the increase of isothermal temperature, the solid volume fraction of semi-solid billet gradually decreases, and the grains grow and spheroidize [28]. Compared with the original structure, the sample is heated at 590℃ for 5 min, and the microstructures are clumped or massive grains formed by dendrite fragmentation because of the lower isothermal temperature and shorter holding time. When the isothermal temperature is increased to 600℃, the homogenization of composition begins to occur in the microstructures, and the eutectic microstructures existing in the intergranular begin to diffuse to the α-Al grains. The α-Al grains partially merge with each other, and the grain size increases. When the temperature rises to 610℃, the microstructure evolution process accelerates. The small grains in the liquid phases begin to spheroidize and grow further. The grain boundaries become smoother and more rounded. At the same time, large clumped grains also begin to break into small particles. It can be noticed that under the same holding time, the higher isothermal time is, the faster the transformation process is. The increase of isothermal temperature can significantly improve the speed of semi-solid microstructure evolution process. This is embodied in the advance of eutectic phase melting time and the increase of the emergence speed of spheroidized particles. However, due to the increase of coarsening power of grain growth, the grains also become larger [29].

It indicates that the evolution rate of semi-solid microstructure is affected by temperature. When the isothermal temperature is low, the driving force of eutectic phases to liquid phases is small. The evolution process of semi-solid microstructures is slow, which also delays the spheroidization rate of α-Al phase with low alloying elements. With the increase of isothermal temperature, the evolution rate of semi-solid microstructures accelerates obviously. When the liquid phases are generated, under the action of interfacial energy and interfacial curvature, small grains will begin to be absorbed by the liquid phases, and large grains will continue to grow and spheroidize, with smooth edges. Thus, the overall solid-liquid boundary area decreases, the system is stable, and the energy decreases [30, 31]. The coarsening and spheroidization of primary grains are based on the remote migration and diffusion of Al and Si atoms. In the absence of convection exerted by an external field in the melt, the migration and diffusion rate of atoms is quite low, resulting in a very low growth rate of α-Al phase. In the process of semi-solid isothermal treatment, as the particles

grow up, the probability of solid particles bumping against each other's edges increases, thus the combining growth of grains is promoted and the grains are more uneven. When two grains with different grain sizes grow into new grains by merging, the newly formed grains become round under the drive of interface energy. However, when two or more grains of similar size merge and grow into new particles, the new particles will not occur spheroidization, but eventually grow into "8" shape or pellet shape. When the melt treatment temperature is too high, the proportion of solid phases is too small, the proportion of liquid phases is too high. This made the forming process will bring too high fluidity and close to casting, which has little significance for the prevention of casting defects.

In the semi-solid isothermal process, the primary dendrites also melt off at the root and the number of grains increases greatly. The eutectic phases with lower melting point tend to be enriched in the dendrite interspaces of the clumps. However, when the temperature of the melt is higher than the solidus temperature, the eutectic phases with lower melting point will become liquid [32], and the clump dendrites will dissociate in the liquid phases. The degree of convexity and concavity of dendrite grain boundaries in contact with the melt liquid phases is different, that is, the radius of curvature is different from each other. According to the influence of curvature radius on melting point, it can be seen that the convex part of grain boundary has small curvature radius, and its melting point is lower [33], so the concave part of grain boundary is further melted and fills in the convex part, and finally generates the spherical grains [34]. Driven by interfacial energy, the small particles suspended in the liquid will tend to have the same degree of concave and convex, and eventually spheroidize. In the process, with the increase of holding time, the grain distribution will be more uniform. This growth mechanism is called Ostwald Ripening mechanism.

The mechanism of grain growth also involves the other mechanism, coalescence of grains, which is that the adjacent primary α-Al phase grains with similar lattice orientation begin to grow together during the holding process. The α-Al grains continuously merge and grow. Due to the inclusion of a small amount of liquid phases during grain consolidation, there are liquid phases in the larger grains after the merger. There is a high liquid rate in the structure, with good fluidity, and the small solid phases in the liquid phases will gradually melt into the liquid phases, so that the liquid fraction will gradually increase. The grains have good roundness, and the primary α-Al grains grow uniformly in all directions and gradually become rounder due to the liquid-solid interfacial tension. There are two reasons for this phenomenon. First, due to the presence of liquid phases, under the action of interface curvature and interface energy, in order to make the solid-liquid interface of the whole system lower and reduce the energy of the system, the small primary α phase grains gradually melt, and the large primary α phase grains grow up and become more rounded. Second, When the liquid fraction is high, it is assumed that the solid-liquid phases are in equilibrium, but the small grains correspond to lower equilibrium melting point, and the large grains correspond to higher equilibrium melting point. Therefore, at the same temperature, the small grains correspond to the liquid phases with lower Si content, while the large grains correspond to the liquid phases with higher Si content, resulting in the diffusion of Si in the liquid phases to the liquid phases on the side of the small grains. At the same time, Al in the liquid phases diffuse to the side of the large grains, causing the continuous melting of the small grains and the continuous growth of the large grains.

Quantative analysis of semi-solid billet fabricated by SSITWA. Fig. 7 shows the point plot of average grain size and average shape factor of semi-solid billet fabricated by SSITWA at different isothermal temperatures and holding times. As shown in Fig. 7(a), when the specimen was heated at different isothermal temperatures, the average grain size generally changes in the same way with the extension of holding time. When the holding time is 590℃, with the increase of holding time, the size of primary α-Al phase increases and then decreases obviously. The average grain diameter

increases gradually from 15 μm at 1 min to 30 μm at 5 min, and further increases to 55 μm at 10 min. Then it decreases to 30 μm at 15 min, followed by a slight decrease to 28 μm at 20 min. This is because in the early stage of semi-solid isothermal treatment, the solid fraction is high, adhesion and merger phenomenon between adjacent grains, like "8" word grains or petal-like grains appear. With the further extension of holding time, the eutectic phases with low melting point between grains melt, and the grain boundary becomes obvious. It is difficult to merge between grains, and the grains begin to spheroidize, which further reduces the free energy and accords with the Ostwald growth mechanism [35]. The average grain size of AlSi7Mg aluminum alloy semi-solid billet fabricated by SSITWA varies in a range of from 15 μm to 65 μm when the isothermal temperature and holding time change.

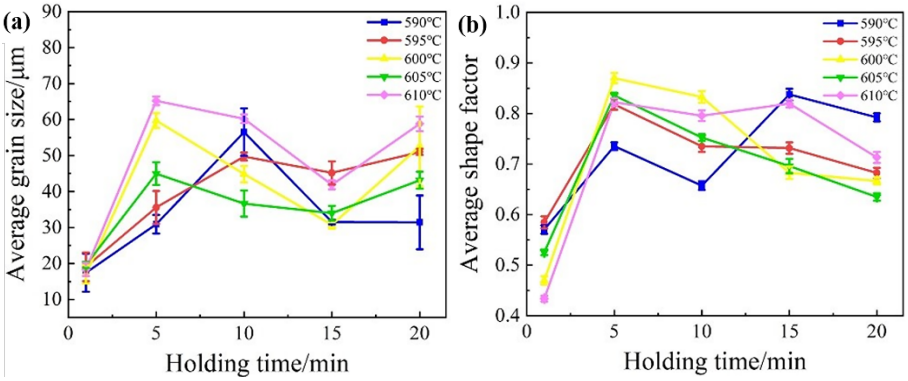

Fig. 7. Point plot of average grain size and average shape factor: (a) Average grain size; (b) Average shape factor.

In the other four temperature parameters, the grain size increases to different degrees when holding time is 20 min compared with holding time of 15 min. This is because when the isothermal temperature is lower, the evolution process of semi-solid microstructure is slower than that when the isothermal temperature is higher. When the holding time is 20 min, it is mainly rosette grains broken into massive or spherical small grains. With the increase of isothermal temperature, the process of microstructures evolution is accelerated. When the holding time is 20 min, the microstructures begin to have different degrees of grain growth or combined growth.

It can be seen from Fig. 7(b) that with the extension of holding time, the average shape factor generally tends to increase first and then decrease. When the holding time is 1 min, the grain sizes of the original dendrites and the grains produced by fragmentation are large and small. The grain edges are irregular, their growth rates are different, and the average shape factor is small. When the holding time reaches 5 min, the grains are gradually rounded and the average shape factor becomes larger. With the further extension of holding time, some grains begin to merge and grow, Some "8" shaped grains or petal-like grains appear with irregular shape, resulting in the decrease of the average shape factor. However, with the extension of holding time to 10 min and 15 min, the liquid phases increase, the grains are isolated, which are not easy to merge and grow, and begin to transform into spherical grains. The shape factor increases at 590℃ and 610℃. The average shape factor decreases at all temperature parameters during the transition from 15 min to 20 min. The average shape factor varies in a range of from 0.65 to 0.85 when the holding time changes from 5 min to 20 min. It illustrates that good spheroidization effect is obtained. As reported by Kiuchi and Kopp [36], a shape factor greater than 0.5 indicates a good spheroidization of semi-solid billets. Compared with other methods in Table 3, including electromagnetic stirring (ES) method [37], cooling slope (CS) method [38], ultrasonic treatment (UT) method [39], strain induced melt activation (SIMA) method [40], rheoforged and semi-solid holding process(RFSSH)

method [40]and equal-channel angular pressing (ECAP) method [41], the results show that the SSITWA method has a good effect on the preparation of AlSi7Mg semi-solid billet.

Table 3. The average grain size and average shape factor from different works.

Aluminum alloy	Method	Average grain size/μm	Average shape factor/μm
AlSi7Mg	SSITWA	15~65	0.65~0.85
A356	ES	113.62~127.25	3.9~5.9
A356	CS	74~105	0.41~0.54
A356	UT	50	0.7
A356	SIMA	70	0.85
A356	RFSSH	100	0.82
A356	ECAP	21~35	-

Energy spectrum analysis of AlSi7Mg aluminum alloy semi-solid billet prepared by SSITWA. Fig. 8 shows SEM point scanning analysis diagram of AlSi7Mg alloy after holding at 600℃ for 5 min. Analysis equipment was Zeiss field emission scanning electron microscope (SUPRA55). Three test points were selected from the area in Fig. 8(a) for element analysis. Spot1 and Spot3 are intragranular, and Spot2 is intergranular. As shown in Fig. 8, the content of Al element in Spot3 is obviously higher than that in Spot1 and Spot2. It is because that the phase in Spot3 is α-Al phase and the phase in Spot1 and Spot2 is eutectic phase consisting of Al and Si elements.

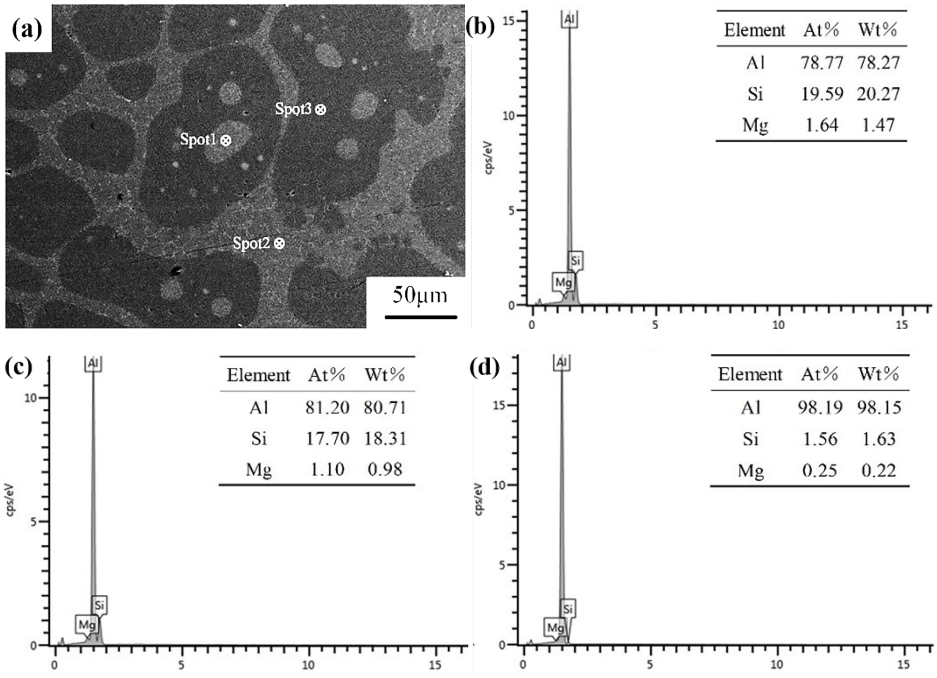

Fig. 8. SEM point scanning analysis diagram of AlSi7Mg alloy held at 600℃ for 5 min: (a) The area being scanned; (b) Spot1 element analysis; (c) Spot2 element analysis; (d) Spot3 element analysis.

Fig. 9 shows the SEM line scanning analysis diagram of the AlSi7Mg alloy after holding at 600℃ for 5 min. Fig. 9(b) lists the variation curves of the contents of main elements Al and Si in

and between grains. It can be seen that Si is mainly enriched in the liquid phase region between grains and ingrains, while Al is relatively evenly distributed, and its content in the non-liquid phase region in grains is slightly higher than that in the liquid phase region between grains and ingrains.

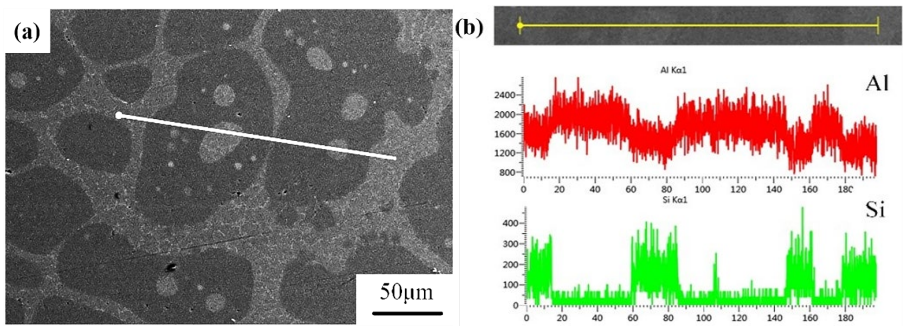

Fig. 9. SEM line scanning analysis diagram of AlSi7Mg alloy held at 600℃ for 5 min.

Fig. 10 shows the SEM map scanning analysis diagram of AlSi7Mg alloy after holding at 600℃ for 5 min. Fig. 10(a)-(f) shows the distribution of Al, Si, Mg, Ti and Fe elements on the selected region. It can be seen from the map scanning results that the eutectic phases first melt and form ingrain droplet and intergranular liquid phases due to its low melting point. In the whole isothermal process, the composition of Al and Si elements is different at different positions. It can be seen from Fig. 10(b) that Al element is distributed inhomogeneously in the whole, especially in the interior of the grains, and the content of Al element in the liquid phase region between grains and inside grains is slightly lower. Si element is obviously enriched in the liquid phase region between grains and inside grains, due to eutectic silicon mainly exists in these two regions. The distribution of Mg element is uniform as a whole, and there is little difference in the distribution within and between grains. The contents of Ti and Fe are small, but they are evenly distributed on the regional surface. The contents of other trace elements and impurity elements are relatively small, which can be ignored under the results of map scanning.

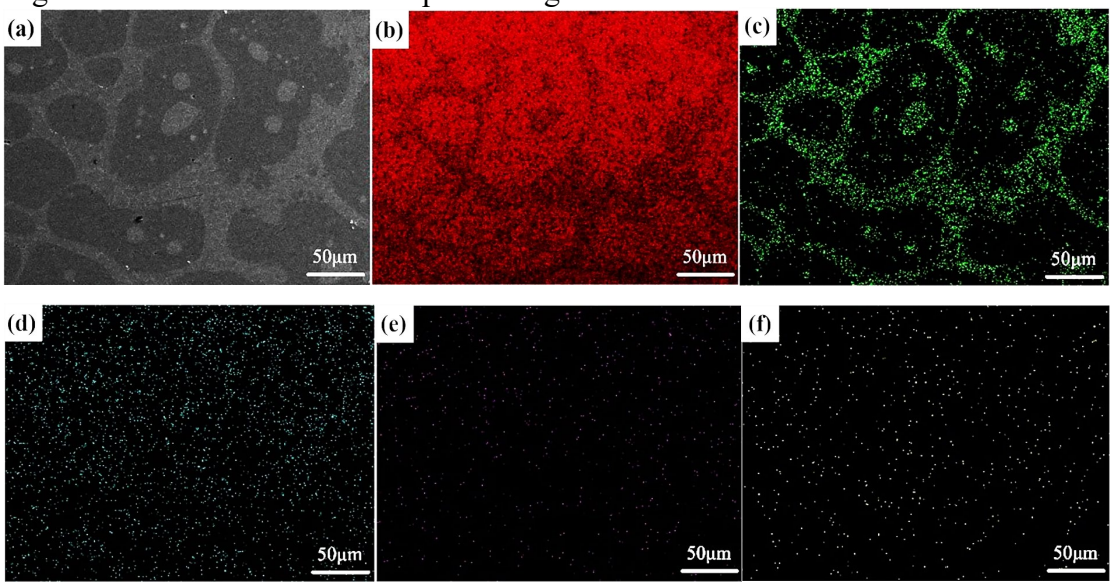

Fig. 10. SEM surface scanning analysis of AlSi7Mg alloy held at 600℃ for 5 min: (a) The area being scanned; (b) Al element; (c) Si element; (d) Mg element; (e) Ti elements; (f) Fe element.

Conclusions

In this paper, semi-solid billet of AlSi7Mg aluminum alloy is fabricated by isothermal treatment in semi-solid temperature range after hot upsetting at 350℃ for 50% deformation degree. The

microstructure evolution during semi-solid isothermal treatment of wrought alloy was investigated. The research conclusions are as follows:

(1) With the increase of holding time in semi-solid isothermal process, the evolution process of primary phase morphology is as follows: dendrite growth → massive or granular → rosette → fragmentary massive or granular → spheroidization → grain growth. Under the same holding time, the higher isothermal temperature can increase the primary grain size and shorten the time of dendrite morphology transformation to granular form.

(2) During the semi-solid isothermal process, the average grain size increases first, then decreases and then increases. The trend of average shape factor increases first, then decreases, then increases and then decreases. The average grain size of AlSi7Mg aluminum alloy semi-solid billet fabricated by SSITWA varies in a range of from 15 μm to 65 μm when the isothermal temperature and holding time change. The average shape factor varies in a range of from 0.65 to 0.85 when the holding time changes from 5 min to 20 min. It illustrates that good spheroidization effect is obtained.

(3) The results of point, line and map scanning show that the content of Al element in α-Al is obviously higher than that in liquid eutectic phase due to different phase. Si element is mainly distributed in the eutectic organization of intergranular, while Mg element has no significant difference in the distribution in and out of grains.

Acknowledgement
This work is supported by the National Natural Science Foundation of China (NSFC) under Grant Nos.U2241232, U2341253 and 52375317 and the National Key R&D Program of China (No.2022YFB3404204).

Data Availability
The raw/processed data required to reproduce these findings cannot be shared at this time due to technical or time limitations.

Conflict of Interest
On behalf of all authors, the corresponding authors state that there is no conflict of interest.

References

[1] H. Yang, W.T. Tian, Metallurgical Structure of A356 Alloy Solidified by Mechanical Stirring, Solid State Phenom. 285 (2019) 183-188.

[2] Y.E. Albarbary, R. Afify, E.H. Mansour, T.S. Mahmoud, M. Khedr, The effect of pre-drilling on the characteristics of friction drilled A356 cast aluminum alloy, J. Manuf. Process. 82 (2022) 646-656. http://dx.doi.org/10.1016/j.jmapro.2022.08.040

[3] N.Z. Liu, B. Jiang, Y.Wang, Z.S.Ji, M.L.Hu, H.Y. Xu, Influence of trace amount chromium on microstructure and corrosion behavior of A356-5vol.%TiB2 alloy, Mater. Lett. 314 (2022) 131798.

[4] S.K. Thandalam, J. Nampoothiri, S. Shalini, T. Thankachan, Microstructure and Wear Characteristics of Nano Y_2O_3 Particles Reinforced A356 Alloy Composites Synthesized Through Novel Ultrasonic Assisted Stir Casting Technique, Trans. Indian Inst. Met. 75 (2022) 417-426. http://dx.doi.org/10.1007/s12666-021-02424-1

[5] P. Nelaturu, S. Jana, R.S. Mishra, G. Grant, B.E. Carlson, Effect of temperature on the fatigue cracking mechanisms in A356 Al alloy, Mater. Sci. Eng. A 780 (2020) 139175. https://doi.org/10.1016/j.msea.2020.139175

[6] V.H. Carneiro, J. Grilo, D. Soares, I. Duarte, H. Puga, The Influence of Precipitation Hardening on the Damping Capacity in Al-Si-Mg Cast Components at Different Strain Amplitudes, Metals 12 (2022) 804. http://dx.doi.org/10.3390/met12050804

[7] S. Zhang, L. Bo, L. Wang, Y.B. Hou, D. Zhao, Effects of thermal-rate treatment and modification of Ce on the microstructure and properties of A356 alloys, J. Phys.: Conf. Ser. 1885 (2021) 022064. http://dx.doi.org/10.1088/1742-6596/1885/2/022064

[8] M. Varmazyar, S. Yousefzadeh, M.M. Sheikhi, Effect of Ni on Microstructure and Creep Behavior of A356 Aluminum Alloy, Met. Mater. Int. 28 (2022) 579–588. http://dx.doi.org/10.1007/s12540-020-00892-6

[9] G.F. Xiao, J.F. Jiang, Y.Z. Liu, Y. Wang, B.Y. Guo, Recrystallization and microstructure evolution of hot extruded 7075 aluminum alloy during semi-solid isothermal treatment, Mater. Charact. 156 (2019) 109874.

[10] J. Liu, Y.S. Cheng, S.W.N. Chan, D. Sung, Microstructure and mechanical properties of 7075 aluminum alloy during complex thixoextrusion, Trans. Nonferrous Met. Soc. China 30 (2020) 3173-3182. http://dx.doi.org/10.1016/S1003-6326(20)65452-8

[11] Y.F. Wang, S.D. Zhao, Y. Guo, K.X. Liu, S.Q. Zheng, Deformation Characteristics and Constitutive Equations for the Semi-Solid Isothermal Compression of Cold Radial Forged 6063 Aluminium Alloy, Materials 14 (2021) 194. https://doi.org/10.3390/ma14010194

[12] H. Negini, A. Rezaei, M. Hajisafari, H. Momeni, Effects of semi-solid thermomechanical processing on microstructure and mechanical properties of Al 2024, Trans. Indian Inst. Met. 72 (2019) 1201-1209. http://dx.doi.org/10.1007/s12666-019-01608-0

[13] Q. Gao, B. Yang, G.S. Gan, Y.J. Zhong, L. Sun, W.Y. Zhai, W. Qiang, S.Q. Wang, Y.X. Lu, Microstructure and Wear Resistance of TiB2/7075 Composites Produced via Rheocasting, Metals 10 (2020) 1068. https://doi.org/10.3390/met10081068

[14] Y.Z. Liu, J.F. Jiang, Y. Zhang, M.J. Huang, Y. Wang, Semi-solid compression of 2A14 alloy with high solid fraction: rheology, constitutive equation and microstructure, J. Mater. Sci. 57 (2022) 16507–16527. http://dx.doi.org/10.1007/s10853-022-07656-0

[15] Y. Liu, M.Q. Gao, Y. Fu, W.R . Li, P. Yang, R.G. Guan, Microstructure Evolution and Solidification Behavior of a Novel Semi-Solid Alloy Slurry Prepared by Vibrating Contraction Inclined Plate, Metals 11 (2021) 1810. https://doi.org/10.3390/met11111810

[16] Y.F. Wang, Y. Guo, S.D. Zhao, Effects of Process Parameters on the Microstructure and Hardness of Semi-Solid AlSi9Mg Aluminum Alloy Prepared by RAP Process, Mater. Trans. 61 (2020) 1731-1739. http://dx.doi.org/10.2320/matertrans.MT-M2020088

[17] M. Jahanbakhshi, S. Nourouzi, R. Naseri, K. Esfandiari, Investigation of Simultaneous Effects of Cooling Slope Casting and Mold Vibration on Mechanical and Microstructural Properties of A356 Aluminum Alloy, Met. Mater. Int. 28 (2022) 1508-1516. https://ui.adsabs.harvard.edu/link_gateway/2022MMI....28.1508J/doi:10.1007/s12540-021-01056-w

[18] L.J. Cao, G.R. Ma, C.X. Wang, Z.J. Chen, J.H. Zhang, Effect of compression ratio on microstructure evolution of Mg–10%Al–1%Zn–1%Si alloy prepared by SIMA process, Trans. Nonferrous Met. Soc. China 31 (2021) 2597-2605. https://doi.org/10.1016/S1003-6326(21)65678-9

[19] J.F. Jiang, Y.Z. Liu, G.F. Xiao, Y. Wang, Thixoforming of Semisolid Slurry with High Fraction Solid Fabricated by Partial Melting of Commerical Wrought Aluminum Alloys, Solid State Phenom. 285 (2019) 210-218.

[20] T.Y. Guan, Z.F. Zhang, M. He, Y.L. Bai, P. Wang, Effects of Annular Electromagnetic Stirring Melt Treatment on Microstructure and Mechanical Properties of 7050 Rheo-Casting, Solid State Phenom. 285 (2019) 219-223.

[21] W.C. Liu, Y. Sun, C. Deng, L.X. Hu, S.J. Yuan, J.Y. Shen, F. Gao, M.Y. Ba, Cu strengthened Al-Si-Cu semi-solid billet fabricated by liquid phase reaction sintering, Mater. Charact. 188 (2022) 11925.

[22] Z.X. Zhang, T.J. Chen, H. Xue, G.L. Bi, Y. Ma, R.G. Guan, Microstructure Evolution of an Al-Si Alloy During Shear-vibration Coupling Sub-rapid Solidification and the Effects of Processing Parameters, Int. J. Metalcast. 17 (2022). http://dx.doi.org/10.1007/s40962-022-00809-6

[23] L.J. Yu, H. Yan, L.X. Xu, L.J. Zhang, Z.B. Liu, Rheological Research of the Semisolid ADC12 Slurry Prepared with High-Energy Ultrasound and Pr/Ce Addition, Trans. Indian Inst. Met. 75 (2022) 495-502.

[24] J.F. Jiang, Y.H. Zhang, Y.Z. Liu, Y. Wang, G.F. Xiao, Y. Zhang, Research on AlSi7Mg Alloy Semi-solid Billet Fabricated By RAP, Acta Metall. Sin. 57 (2021) 703-716. http://doi.org/10.11900/0412.1961.2020.00254

[25] P.K. Seo, C.G. Kang, The effect of raw material fabrication process on microstructural characteristics in reheating process for semi-solid forming, J. Mater. Process. Technol. 162-163 (2005) 402-409. https://doi.org/10.1016/j.jmatprotec.2005.02.012

[26] Z. Liu, K. Cao, H.B. Xu, M.Y. Huang, Evolution Characteristics of Primary Phase in A356 Al Alloy during Isothermal Holding in Solid-Liquid Phase Region, Adv. Mater. Res. 421 (2012) 39-42. http://dx.doi.org/10.4028/www.scientific.net/AMR.421.39

[27] S.B. Hassas Irani, A. Zarei-Hanzaki, B. Bazaz, A.A. Roostaei, Microstructure evolution and semi-solid deformation behavior of an A356 aluminum alloy processed by strain induced melt activated method, Mater. Des. 46 (2013) 579-587. http://dx.doi.org/10.1016/j.matdes.2012.10.041

[28] W. Khalifa, S. El-Hadad, Y. Tsunekawa, Microstructure characteristics and tensile property of ultrasonic treated-thixocast A356 alloy, Trans. Nonferrous Met. Soc. China 25 (2015) 3173-3180. https://doi.org/10.1016/S1003-6326(15)63949-8

[29] A. Mahdavi, M. Bigdeli, M. Hajian Heidary, F. Khomamizadeh, Study of Microstructural Evolution and Phase's Morphology after Partial Remelting in A356 Alloy, Solid State Phenom. 141-143 (2008) 367-372. http://dx.doi.org/10.4028/www.scientific.net/SSP.141-143.367

[30] H. Arami, R. Khalifehzadeh, H. Keyvan, F. Khomamizadeh, Effect of predeformation and heat treatment conditions in the SIMA process on microstructural and mechanical properties of A319 aluminum alloy, J. Alloy. Compd. 468 (2009) 130-135. http://dx.doi.org/10.1016/j.jallcom.2008.01.020

[31] K. Wang, Z.M. Zhang, H. Wen, D. Xia, W.J. Sun, Microstructural evolution of a fine-grained 7075Al alloy processed by friction stir process during partial remelting, Mater. Charact. 121 (2016) 1-8. https://doi.org/10.1016/j.matchar.2016.09.029

[32] S. Ashouri, M. Nili-Ahmadabadi, M. Moradi, M. Iranpour, Semi-solid microstructure evolution during reheating of aluminum A356 alloy deformed severely by ECAP, J. Alloy. Compd. 466 (2008) 67-72. https://doi.org/10.1016/j.jallcom.2007.11.010

[33] Y. Hu, F. Liu, L.Z. Zhao, Y.C. Tang, H.T. Jiao, Microstructural Evolution and Mechanical Properties of Semi-Solid $Al_{15}Mg_{45}Li_{39}Ca_{0.5}Si_{0.5}$ Light-Weight High Entropy Alloys Fabricated by Isothermal Heat Treatment, Met. Mater. Int. 29 (2023) 1489-1497. https://ui.adsabs.harvard.edu/link_gateway/2023MMI....29.1489H/doi:10.1007/s12540-022-01303-8

[34] C.P. Wang, Z.J. Tang, H.S. Mei, L. Wang, R.Q. Li, D.F. Li, Formation of spheroidal microstructure in semi-solid state and thixoforming of 7075 high strength aluminum alloy, Rare Met. 34 (2015) 710–716. http://dx.doi.org/10.1007/s12598-013-0123-0

[35] Y. Hu, S.Q. Fu, L.Z. Zhao, D.H. Wang, F. Liu, Microstructure evolution of semi-solid Mg2Si/A356 composites during remelting process, China Foundry 17 (2020) 384-388. http://dx.doi.org/10.1007/s41230-020-9158-7

[36] M. Kiuchi, R. Kopp, Mushy/Semi-Solid Metal Forming Technology – Present and Future, CIRP Ann. Manuf. Technol. 51 (2002) 653-670. https://doi.org/10.1016/S0007-8506(07)61705-3

[37] J.S. Roh, M. Heo, C.K. Jin, J.H. Park, C.G. Kang, Effect of Current Input Method on A356 Microstructure in Electromagnetically Stirred Process, Metals 10 (2020) 460. https://doi.org/10.3390/met10040460

[38] A. Kolandooz, S.A. Dehlzordi, Effects of important parameters in the production of Al-A356 alloy by semi-solid forming process, J. Mater. Res. Technol. 8 (2018) 189-198. http://dx.doi.org/10.1016/j.jmrt.2017.11.005

[39] W. Khalifa, S. El-Hadad, Y. Tsunekawa, Microstructure characteristics and tensile property of ultrasonic treated-thixocast A356 alloy, Trans. Nonferrous Met. Soc. China 25 (2015) 3173-3180. http://dx.doi.org/10.1016/S1003-6326(15)63949-8

[40] A. Dodangeh, M. Kazeminezhad, H. Aashuri, Effects of cold severe plastic deformation and heating on dendritic and non-dendritic structures: A356 alloy, Int. J. Cast Met. Res. 27 (2014) 312-320. http://dx.doi.org/10.1179/1743133614Y.0000000116

[41] M. Moradi, M. Nili-Ahmadabadi, B. Poorganji, B. Heidarian, T. Furuhara, EBSD and DTA Characterization of A356 Alloy Deformed by ECAP During Reheating and Partial Re-melting, Metall. Mater. Trans. A 45 (2014) 1540-1551. http://dx.doi.org/10.1007/s11661-013-2093-0